Anadolu Üniversitesi Bilim ve Teknoloji Dergisi A- Uygulamalı Bilimler ve Mühendislik
Anadolu University Journal of Science and Technology A- Applied Sciences and Engineering

Year: 2018
Volume: 19
Number: 2
Page: 468 - 483
DOI: 10.18038/aubtda.328064

ANADOLU UNIVERSITY

PLASMA MODIFIED WO_3 HYBRIDS WITH ALTERED DONOR GROUPS FOR FLEXIBLE ELECTROCHROMIC APPLICATIONS

Esin EREN [1,*], Ceyda ALVER [1], Ayşegül UYGUN ÖKSÜZ [1]

[1] Department of Chemistry, Süleyman Demirel University, Faculty of Arts and Science, 32260 Isparta, Turkey

ABSTRACT

This study reports on the preparation of hybrids of tungsten trioxide/polythiophene (WO_3/PTh) and tungsten trioxide/polyfuran (WO_3/PFu) using a rotating capacitively-coupled radio frequency (rf) plasma process. The prepared hybrid characteristics were measured using scanning electron microscopy-energy dispersive X-ray spectroscopy (SEM-EDS) and X-ray diffraction analysis (XRD). WO_3, WO_3/PTh, and WO_3/PFu thin films were deposited onto flexible substrates using an electron beam evaporation technique for high electrochromic performance purposes. The effect of thiophene and furan moieties on the optical and electrochromic properties of flexible hybrid-based ECDs was investigated using optical and electrochemical measurements. The WO_3/PTh-based ECD, in particular, showed marked improvements in cathodic electrochromism over WO_3-based ECD: an optical contrast of 33% at 750 nm, faster switching times (bleaching time: 1.63 s, coloration time: 0.41 s), and a coloration efficiency of 502 cm^2/C.

Keywords: Flexible electrochromic, Hybrid, Plasma modification, Tungsten trioxide

1. INTRODUCTION

Flexible electronics are a developing class of electronics that allow a vast range of applications such as bendable cell phones, flexible displays, electronic skin, wearable electronics, sensors, bio-integrated therapeutics, real-time health monitoring, etc. [1, 2]. Of all the flexible electronics, flexible electrochromic devices (ECDs) have attracted the most attention because of their multifunctional properties. Flexible ECDs can reversibly change their color via an applied external voltage as in the traditional ECDs and deform freely in a diversity of forms, allowing them to have specific applications in flexible electrochromic display, curved windows, and military camouflage [1]. Since the flexible ECDs using tungsten trioxide (WO_3) films were developed in 1995, a vast range of inorganic and organic materials have been investigated with respect to their compatibility with flexible substrates such as poly (ethylene terephthalate) (PET) substrates [3].

Among the various inorganic materials for electrochromics, WO_3 gains special interest due to its robust behavior [4]. However, inorganic EC materials such as WO_3 generally have slow switching times and poor flexibility compared to organic EC materials; this prevents their application in high performance flexible ECDs [5]. As the literature shows, WO_3, in its fully oxidized state, shows low conductivity as a semiconductor [6, 7]. One way to overcome the above problems is the fabrication of a hybrid, an inorganic material with an organic material (i.e. conducting polymer) that is electrically conductive under positive potentials (p-type) and has fast switching times [4, 6-8]. The discovery of polyacetylene $(CH)_x$ in 1977 started the conductive polymer era [9-12]. Since then, progress in heteroaromatic conducting polymers such as polythiophene (PTh) and polyfuran (PFu) have been comprehensively investigated due to low cost, ease of processing, and electronic and optical properties [13].

Since then, much scientific research has been focused on ECDs based on inorganic EC materials and organic conducting polymers. Generally, inorganic/organic hybrid materials create a natural interface

*Corresponding Author: eso_eren@yahoo.com.tr
Receiving Date: 12 July 2017 Publishing Date: 29 June 2018

between the two worlds of materials science. In this field, many difficulties in preparing inorganic-organic hybrid combinations that keep or increase the best features of each of the components while eliminating or decreasing their particular imperfections has been overcome [14]. Kim et al. reported on the production of organic-inorganic hybrid materials consisting of WO_3 and P3HT (poly(3-hexylthiophene)) that displayed improved electrochemical and electrochromic features compared to pristine WO_3 and P3HT [15]. Nguyen et al. developed a hybrid film that included tungsten oxide and poly (3,4-ethylenedioxythiophene):polystyrene sulphonate (WO_3–PEDOT:PSS) using one-step inkjet printing from an office inkjet printer. The inkjet-printed WO_3-PEDOT:PSS thin films demonstrated a remarkable enhancement of cathodic electrochromism over WO_3 films: an optical contrast of 20% at 550 nm (visible region) and 35% at 900 nm (infrared region along with a switching time of 5.67 s/0.30 s in their colored/bleached state, and an electrochromic coloration efficiency of 27.86 cm^2/C at 550 nm and 69.64 cm^2/C at 900 nm [16]. Recently, Gaikwad et al. prepared a hybrid film including WO_3 on an ITO substrate using the electrodeposition method followed through the deposition of polypyrrole (PPy) layer using the chemical bath deposition method. Their results evinced that the disordered morphology of WO_3/PPy offered wonderful electrochemical durability with improved optical density [17]. Therefore, conducting polymers incorporated with WO_3 can be a useful way to develop the electrochromic features of raw WO_3 materials for electrochromic applications.

In this study, both WO_3/PFu and WO_3/PTh hybrids were prepared via the rf rotating plasma modification method. For the use of the rf rotating modification method, the preparation of hybrids played a significant role because of solvent-free, nontoxic, and well-controlled deposition [4, 18, 19]. To the best of our knowledge, there is no report on the preparation of WO_3/PFu and WO_3/PTh hybrids using the rf rotating plasma modification method for flexible electrochromic applications. The hybrid films were obtained using electron beam evaporation. The effect of thiophene and furan donor groups on WO_3-based hybrid flexible ECDs was evaluated in detail. Furthermore, optical contrast, coloration efficiency, switching time, and stability were analyzed to compare with the performance of flexible solid-state ECDs.

2. EXPERIMENTAL

2.1. Materials

WO_3 powder (Sigma Aldrich, 99.9%), furan (Fu, ≥99%, Sigma Aldrich), thiophene (Th, ≥99%, Sigma Aldrich), lithium perchlorate ($LiClO_4$, Sigma-Aldrich), poly (methyl methacrylate) (PMMA, (Alfa Aesar), propylene carbonate (PC, Sigma-Aldrich), and acetonitrile (ACN, Sigma-Aldrich) were used as received. ITO-coated PET substrates (sheet resistance of 80- 100 Ω /sq, 25 micrometer thickness) were purchased from the Teknoma Company (Turkey) and were cleaned with ethanol prior to use.

2.2. Preparation of WO_3/PTh, WO_3/PFu Hybrid Powders

The reactor used for plasma coating is a capacitively coupled 13.56 MHz radio-frequency (RF) rotating plasma installation [18]. Dry WO_3 powders were homogeneously dispersed into a cylindrical chamber. The vacuum pressure was dropped 5 Pa (37.50 mTorr) using a vacuum pump. The monomer vapors were sent into the rotating chamber, and the plasma was ignited and maintained during the reaction time. The experimental parameters used during the plasma treatment are as follows: RF-power, 40 W, and a deposition time of two hours.

2.3. Thin Film Deposition and Construction of ECDs

WO_3 and hybrid powders were ground in an agate mortar to obtain homogenous mixed powders. Afterward, the mixed powders were pressed into pellets using a steel die of 13 mm diameter in a hydraulic press under a pressure of 15 MPa. Both WO_3 and hybrid films were prepared onto indium tin

oxide (ITO) coated PET films by the electron beam evaporation method. The pelletized hybrid powders and WO_3 targets were used as evaporation materials and were heated using an electron beam that was collimated from the dc heated cathode, a tungsten filament. The distance between the target area and the rotating panel substrate was 60 cm. The optimized experimental parameters employed in this study are as follows: filament current, 33 A; voltage, 6 kV; and base pressure, 7 x 10^{-6} Torr. The electrochromic film thicknesses onto conductive PET film were controlled using an Inficon SQM-160 model thin film deposition monitor during deposition. The QCM film thickness was calibrated with cross-sectional SEM images.

The gel electrolyte solution used for the flexible ECDs consisted of acetonitrile (ACN), poly (methyl methacrylate) (PMMA), propylene carbonate (PC), and lithium perchlorate ($LiClO_4$) in the ratio of 70:7:20:3 by weight, which is similar to that described in the article [20]. The configurations of the single type ECDs are similar to those in the literature [4, 8, 18, 20]. The active area of the ECD was 3.5 cm^2.

2.4. Characterization

The Gamry PCl4/300 model potentiostat was used for the electrochemical studies. A computer-controlled setup of HR4000 (Ocean Optics, Dunedin, FL, USA) spectrophotometer was employed with a wavelength range of 400 to 900 nm for transmission measurements of solid-state devices. The scanning electron microscopy-energy dispersive X-ray spectroscopy (SEM-EDS) and cross-sectional images were acquired using FEI Quanta FEG 250. X-ray diffraction (XRD) analyses were performed on a Bruker D8 Advance diffractometer with CuKα radiation (λ: 1.54 Å). The diffraction data was recorded for 2θ angles between 10^o and 90^o.

3. RESULTS AND DISCUSSION

3.1. Characterization Results of Hybrid Powders

Plasma polymerization is a convenient technique to deposit thin films on diverse substrates. Moreover, this technique provides good barrier features and good adhesion on substrate surfaces. It is an environmentally friendly method due to the solvents-free requirement and the low temperature of process. This method diminishes the number of processes because it integrates cleaning, the etching of the substrate, and the deposition of the coating, in one process [4, 18, 19, 21, 22]. Plasma polymerization is achieved by introducing organic monomer precursors (vapor) into a plasma reactor leading to the uniform deposition of so-called plasma polymers on the surface of WO_3 powder substrates. In the plasma reaction chamber, the WO_3 surface can be irradiated via the plasma discharge and form a few species including negative ions. The negatively charged WO_3 surface can be combined with the free radicals or positive charges that originated from the monomer, leading to the formation of hybrid powders. As a result, the polymers were formed as thin films adhered to WO_3 powders [18, 19]. The proposed mechanism for the coordination of a conducting polymer with inorganic material is shown in our study [18].

The surface morphological study of untreated WO_3 powder and the prepared hybrid powders (WO_3/PTh, WO_3/PFu) using rf rotating plasma modification method was evaluated using a scanning electron microscope (SEM). The surface morphological images of WO_3 and the hybrid powders are represented in Figure 1a–c. The surface morphology of WO_3 powder revealed spherical close-packed nanograins with different particle sizes (Figure 1a). The surface morphology of all hybrid powders varied slightly from each other, and the shape of nanograins did change significantly. Some voids between the hybrid nanoparticles at the surface can be observed in Figure 1b–c. The enhanced adhesion will efficiently improve the interaction between WO_3 and conducting polymers and facilitate the energy dissipation influence caused by polymers during the crack propagation process which

would greatly influence the fracture toughness of the coating [23]. Moreover, the nanograins became more compact. It was also observed that plasma-polymerized polymer contributed to rougher surfaces when compared to pure WO_3. From this result, it can be assumed that the plasma polymerization formed mainly in the gas phase. In other words, nanoparticles can occur in the gas phase and then be deposited on the WO_3 powders [24].

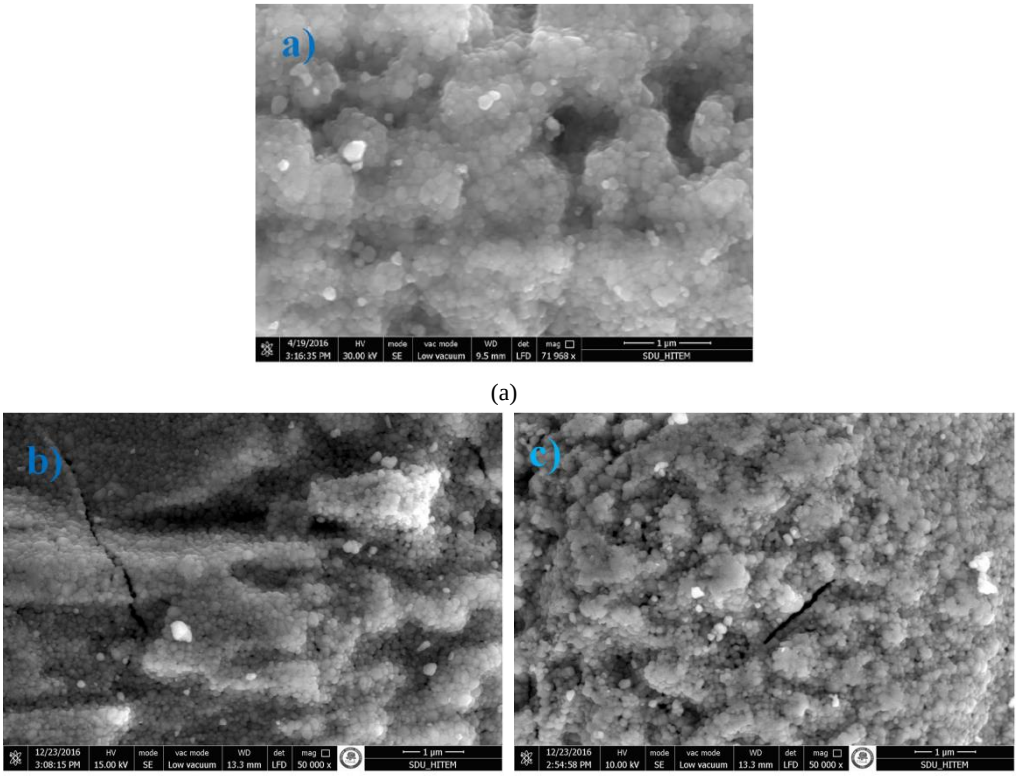

(a)

(b) (c)

Figure 1. SEM images of powders of a) WO_3, b) WO_3/PTh, c) WO_3/PFu.

In addition, an energy dispersive X-ray spectroscopy (EDS) analysis of hybrid powders was performed to demonstrate successful hybrid formation (Table 1). The EDS analysis of pure WO_3 powder shows a tungsten atomic percentage of 29% and an oxygen atomic percentage of 71%. After the hybridization step, a corresponding decrease in the atomic percentages of W and O elements was observed. Furthermore, the presence of both PTh and PFu was confirmed via EDS analysis which showed the additional carbon elements at a 31% ratio and a 31.8% ratio for WO_3-PFu hybrids and WO_3-PTh hybrids, respectively. The EDS result of the WO_3/PTh hybrid powder also indicated an additional sulfur element at 0.4% ratio.

Table 1. Elemental compositions of WO_3 and WO_3/PTh, WO_3/PFu powders

Samples	at. % ratio			
	Tungsten	Oxygen	Carbon	Sulfur
WO_3	29	71	-	-
WO_3/PTh	13.8	54	31.8	0.4
WO_3/PFu	16	53	31	-

Figure 2 shows the XRD patterns of the pure WO_3, WO_3/PTh, and WO_3/PFu powders. All the diffraction peaks of WO_3 are well matched with the standard peaks of the monoclinic WO_3 phase (PCPDS No. 00-024-0747). The XRD analysis results of all the hybrids show that there is little

difference between the curves with regard to the shape and position of diffraction peaks with the addition of the polymer. As seen in the XRD patterns of WO_3/PTh and WO_3/PFu, the small peaks at ~20°C are characteristic peaks for conducting polymers [25-27]. Results imply that the polymer coating on the WO_3 did not have a negative influence on their crystallinity [19, 28, 29].

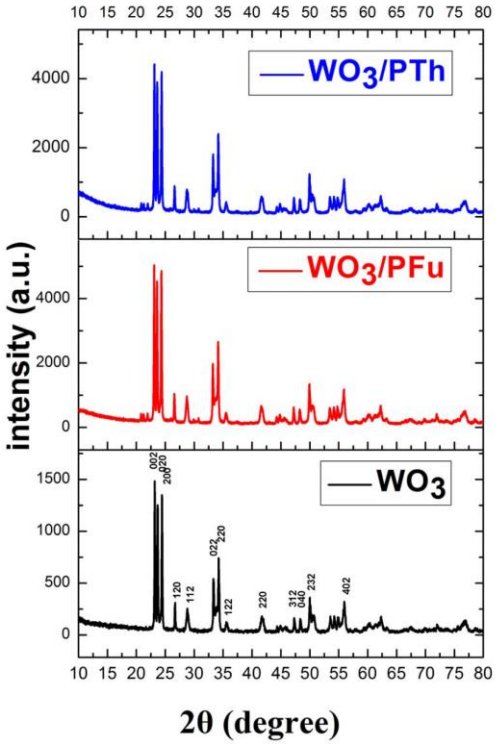

Figure 2. XRD patterns of WO_3, WO_3/PTh and WO_3/PFu powders.

3.2. SEM Results of the Hybrid Films

The surface morphological images of WO_3, WO_3/PTh, WO_3/PFu films on conductive flexible substrate are shown in Figure 3a-c. As seen from Figure 3a, WO_3 thin films are smooth without cracks. Moreover, the surfaces of the thin films have small aggregated WO_3 nanoparticles. Hybrid films show small and spherical nanograins homogeneous distributed all over the substrate surfaces. The cross sections of the WO_3, WO_3/PTh, and WO_3/PFu films grown on ITO coated PET film with 388, 305, 348 nm in thickness respectively were measured with SEM, and the results are presented in Figure 3d-f. Figure 3g-i shows the SEM images of WO_3, WO_3/PTh, and WO_3/PFu films after repeating chronoamperometry measurements during 1000 cycles against an applied cyclic potential of ± 2 V. The results presented in Figure 3g-i is an indication that a degradation does not occurs. Moreover, the SEM images confirmed that all deposited films adhered well onto conductive films.

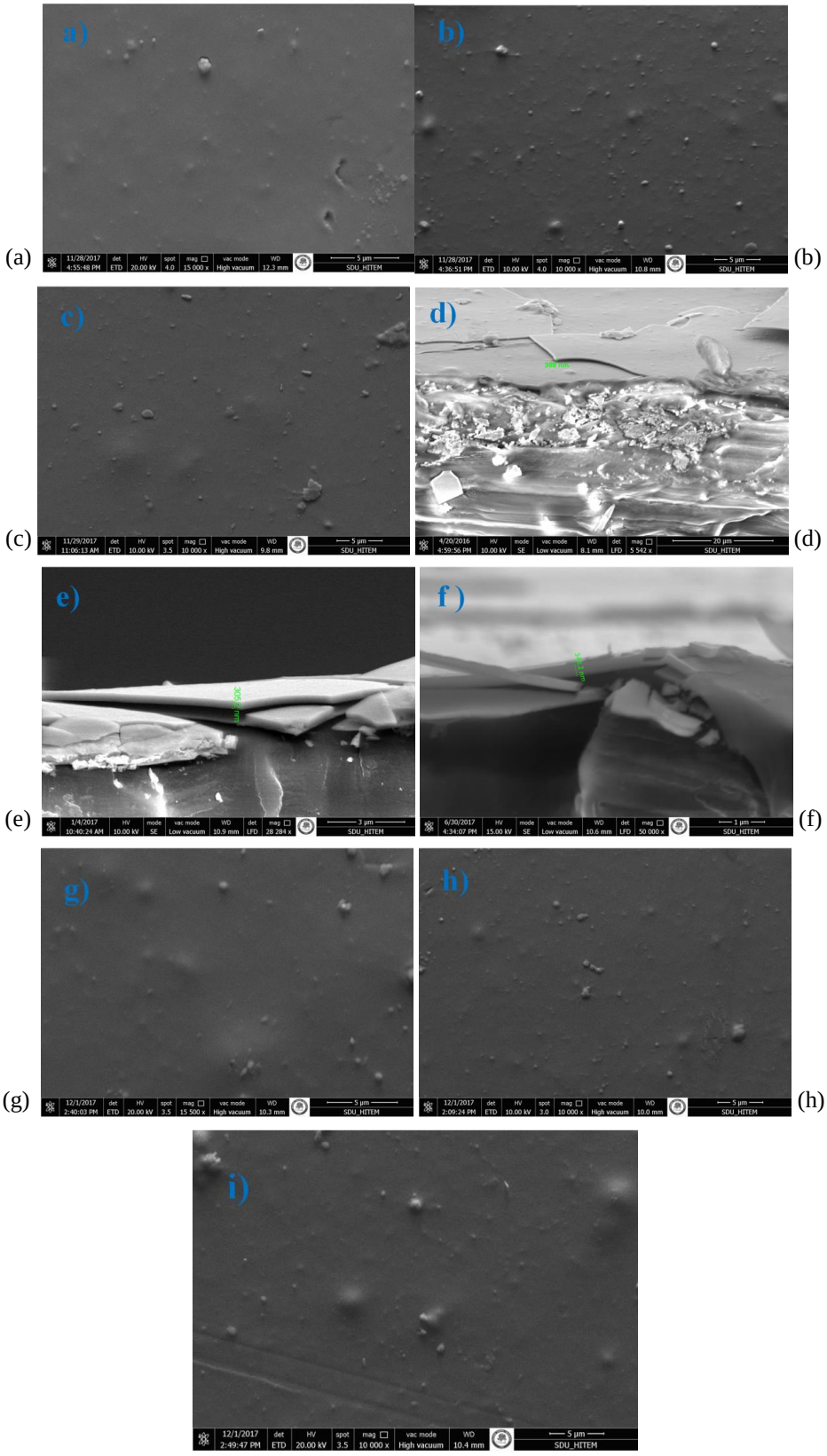

Figure 3. SEM images of films of **a)** WO_3, **b)** WO_3/PTh, **c)** WO_3/PFu, cross section of **d)** WO_3, **e)** WO_3/PTh, **f)** WO_3/PFu before, and **g)** WO_3, **h)** WO_3/PTh, **i)** WO_3/PFu after repeating chronoamperometry measurements.

3.3. ECDs Results

To understand the optical properties of ECDs, the optical transmittance spectra of solid-state devices under + 2 V and -2 V were investigated. Figure 4a-c displays the transmittance spectra within the wavelength range from 400 to 900 nm of all ECDs in their colored and bleached states (applied voltage of -2 V and +2 V, respectively). Optical contrasts were calculated using the differences in transmittance of ECDs between the colored and bleached states at a certain wavelength (750 nm). A transmittance modulation of 17% was observed at 750 nm for WO_3-based ECD. All hybrids exhibited higher optical contrasts, 33% (WO_3/PTh) and 28% (WO_3/PFu), compared to WO_3 (17%) at 750 nm (see Figure 4b-c). The enhanced optical contrast can be attributed to their complementary and synergistic effects [18, 20]. For the thiophene-containing hybrid, a better optical contrast value (33% at 750 nm) was obtained than from the one containing furan. These results are also consistent with the results of Akpinar et. al. Their electrochromic studies show that the increased optical contrast values (40% at 630 nm, 65% at 1230 nm) were achieved for thiophene-containing copolymer when compared to furan-containing copolymer [30].

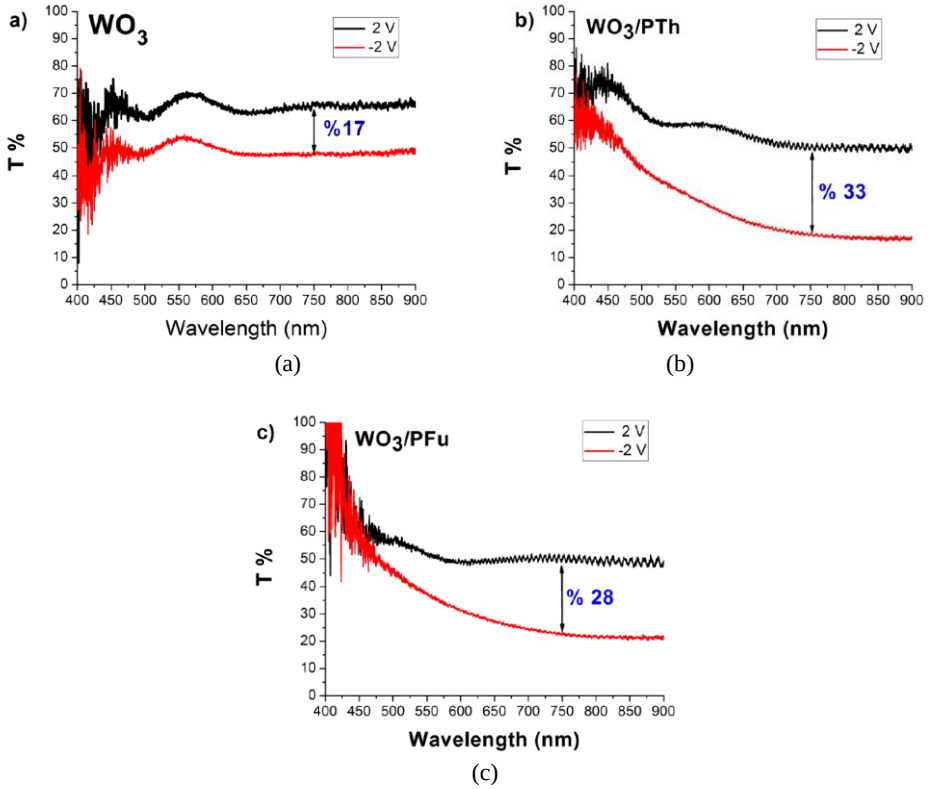

Figure 4. Transmittance change of electrochromic device (ECD) based on a) WO_3, b) WO_3/PTh, c) WO_3/PFu using ACN:PC:PMMA:$LiClO_4$ gel electrolyte for applied potentials of ±2 V.

The color of both WO_3 and hybrid-based ECDs changed from blue (colored state) to transparent (bleached state). Upon the application of -2 V, the color exhibited by the ECDs was blue as a result of WO_3 or hybrid reduction and simultaneous Li^+ insertion. During bleaching +2 V was applied, and the ECDs returned the transparent color, corresponding to the reverse process, i.e. WO_3 or hybrid oxidation and Li^+ deinsertion [8, 20, 31, 32]. Figure 5a-b and Figure 6a-b display the bleached and colored states (applied voltages of +2 V and -2 V, respectively) of WO_3/PTh-based ECD and WO_3/PFu-based ECD, respectively.

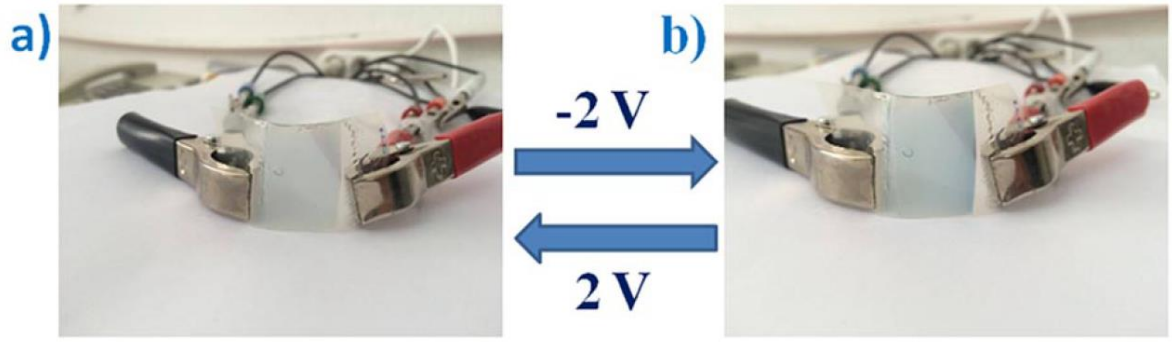

(a) (b)

Figure 5. Photographs of the WO_3/PTh-based ECD in the two extreme states (a) in its bleached state at +2 V (b) in its colored state at -2 V.

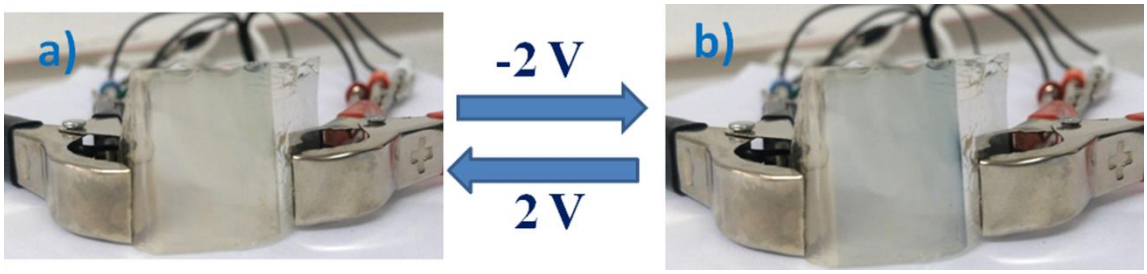

(a) (b)

Figure 6. Photographs of the WO_3/PFu-based ECD in the two extreme states (a) in its bleached state at +2 V (b) in its colored state at -2 V.

Response time is a significant parameter with which to measure the speed in which electrochromic devices change between a colored state and a bleached state by applying a small electric difference [33]. In our electrochromic study, the amperometric i-t curve was used to characterize the response time of the electrochromic devices based on WO_3, WO_3/PTh and WO_3/PFu (Figure 7). The EC response time was calculated at the level of 90% of the full current density switch [34-38]. Response times are listed in Table 2. For the WO_3/PTh-based ECD, the DC voltage steps were applied from -2 V to +2 V; subsequently, the response time for bleached and colored states were calculated as 1.63 and 0.41 s, which are faster than those of WO_3-based ECD (τ_b(s):3.04 s and τ_c(s):0.88 s). This result shows that charge transport is easier. Moreover, the improved EC features can be attributed to the combination of prominences of both materials [39]. Kim et al. prepared the formation of WO_3 nanoporous layers followed by a spin coating of P3HT (poly 3-hexylthiophene). Their results showed that the P3HT/WO_3 exhibited τ_b(s)=5.1 s and τ_c(s)=1.3 s [15]. Moreover, the WO_3/PTh-based ECD displayed a faster switching time than the WO_3/PFu-based ECD (τ_b(s)=2.23 s and τ_c(s)=1.08 s), which indicates a fast electronic state transition [40].

Table 2. Electrochromic parameters of all solid-state devices based on WO_3, WO_3/PTh, and WO_3/PFu films.

	Optical Contrast (% T)	**ΔOD**	**CE (cm^2/C)**	**τ_b(s)**	**τ_c(s)**	**$\Gamma_{(\lambda)}$ ($cm^2C^{-1}s^{-1}$)**
WO_3	17	0.13	85	3.04	0.88	43
WO_3/PTh	33	0.45	502	1.63	0.41	492
WO_3/PFu	28	0.34	374	2.23	1.08	226

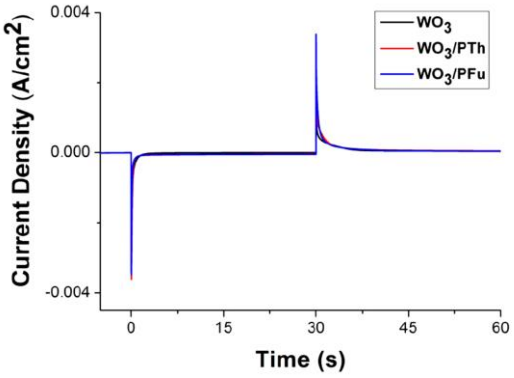

Figure 7. The chronoamperometric response recorded at a potential step of -2V and + 2 V for a time step of 30 s.

The optical absorption of a thin layer is identified by a dimensionless quantity called optical density (OD). The change in ΔOD of WO_3, WO_3/PTh, and WO_3/PFu-based ECDs at 750 nm, in their colored and bleached states, was calculated using the following equation [17]

$$\Delta OD = log \frac{T_b}{T_c}, \quad (1)$$

where T_b and T_c are the transmittances of thin films in bleached and colored states, respectively.

Another important aspect of electrochromism is coloration efficiency (CE) for comparing different electrochromic materials [37]. The CE shows the change in optical density (OD) as a function of injection/ejection of electronic charge, i.e. the amount of charge required for a change in optical modulation. CE can be calculated using the following equation (2) [37]

$$CE = \frac{\Delta OD}{Q} \quad (2)$$

where ΔOD is the change of optical density measured at a wavelength of 750 nm, and Q is the charge density (Ccm^{-2}). The CE and ΔOD calculated for all ECDs are given in Table 2. The coloration efficiency value of WO_3-based ECD was found to be 85 cm^2/C. WO_3-PTh and WO_3-PFu-based ECDs have a CE values of 502 and 374 cm^2/C, respectively. Thus, we have demonstrated that the hybrid systems exhibit improved electrochromic properties, in particular, remarkably enhanced coloration efficiency compared with that of theWO_3 system. The enhancement was ascribed to a combination of donor and acceptor systems [41]. The highest CE of a WO_3/PTh-based ECD shows the large optical modulation with a small charge insertion [4]. Moreover, the rf plasma hybridization approach can boost EC materials performance [4]. Dulgerbaki et al. presented a study on the electrochromic device (ECD) applications of poly(3,4-ethylenedioxythiophene)/tungsten oxide (PEDOT/WO_3) hybrid nanofibers prepared via both electrochemical methods, ionic liquid media and electrospinning. Among all electrochromic devices, the highest coloration efficiency was obtained as 363.72 cm^2/C for PEDOT/WO_3/1-butyl-3 methylimidazolium hexafluorophosphate (BMIMPF6) based electrochromic devices [38]. Furthermore, our results show that the electrochromic performance is better when compared to that of some published studies based on WO_3 hybrids as electrochromic material (Table 3).

Table 3. Comparison of electrochromic properties of WO_3 hybrids

Samples	Preparation Method	Optical Contrast (% T)	CE (cm^2/C)	τ_b(s)	τ_c(s)	Ref
WO_3/PTh	Rf rotating plasma modification & electron beam evaporation methods	33	502	1.63	0.41	This Work
WO_3/P3HT	electrochemical anodization & spin coating methods	-	-	5.1	1.3	[15]
WO_3/PANI	a self-assembly technique and chemical oxidative polymerization.	34.9	40.6	0.8	0.2	[42]
WO_3/PPy	Electrochemical polymerization	33.25	227.89	13.5	16.2	[20]

Repeating chronoamperometry (CA) was used to analyze the stability of ECDs during 1000 cycles at atmospheric conditions. Figure 8a-i shows the current of the ECDs responding to a cyclic potential ± 2 V with the time interval set to 1s. Chronoamperometric measurements were repeated for each of two hours. The obtained changes in current density were listed in Table 4. After the 1000th cycle, the WO_3, WO_3/PTh, and WO_3/PFu-based ECDs retained ~60%, 98%, 72% of the initial current density at 1.25 s during the first measurement. The figures pointed out that WO_3/PTh-based ECD exhibits more stability in electrochemical activity when compared to other ECDs. After the 1000th cycle, the change in current density was obtained as ~2%, 19%, 23% for WO_3/PTh-based ECD at 1.25 s during first, second, and third measurements, respectively.

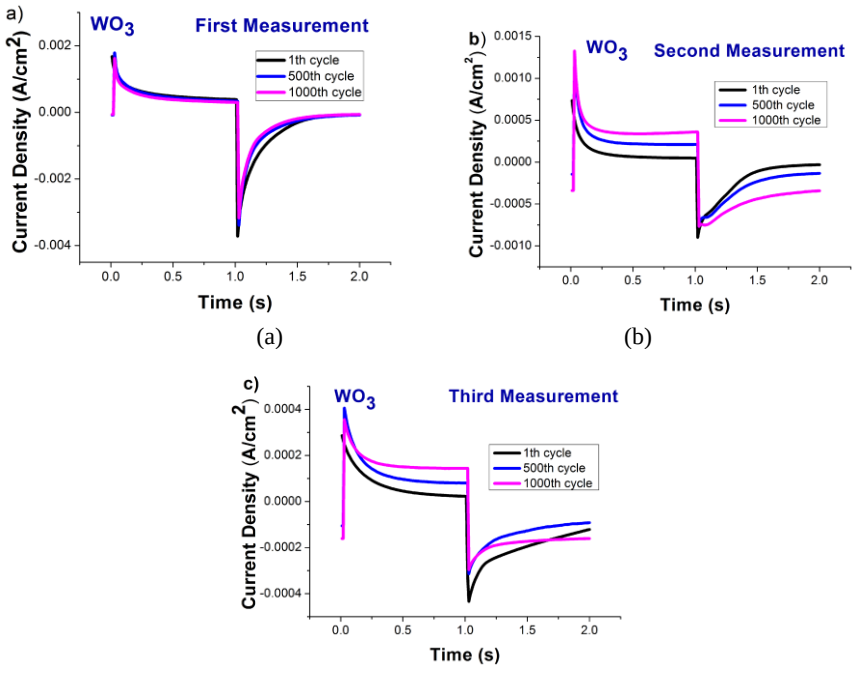

(a) (b)

(c)

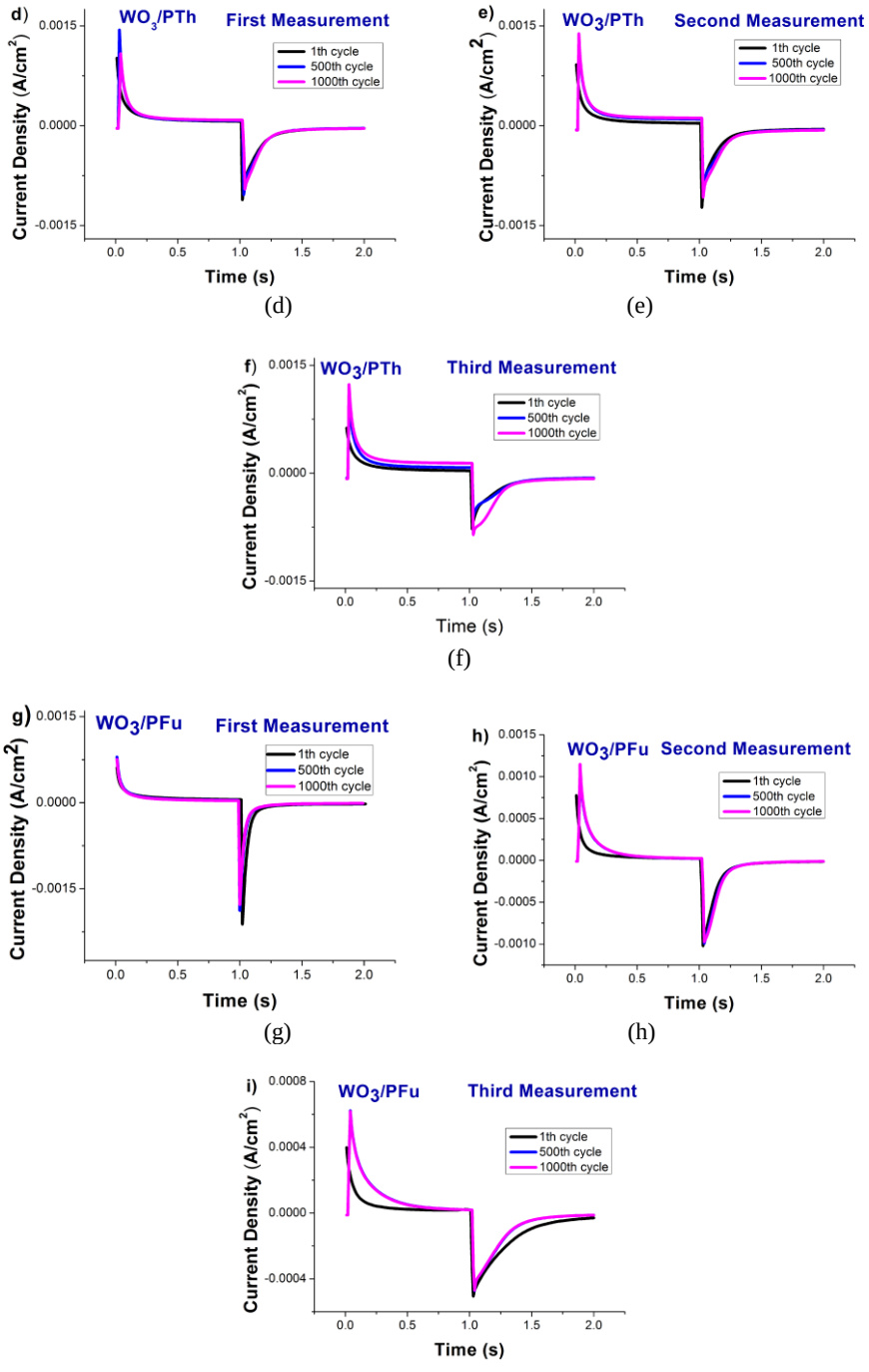

Figure 8. Chronoamperometric measurements of ECDs including a-c) WO_3, d-f)WO_3/PTh, g-i) WO_3/PFu film during 1000 cycles against an applied cyclic potential of ± 2 V with a time step of 1 s.

Table 4. The obtained percent of the changes in current density using chronoamperometric measurements of ECDs at 0.25 s and 1.25 s.

	First Measurement		**Second Measurement**		**Third Measurement**	
	The percent of the change in current density (%)		The percent of the change in current density (%)		The percent of the change in current density (%)	
Sample	**Time (0.25 s)**	**Time (1.25 s)**	**Time (0.25 s)**	**Time (1.25 s)**	**Time (0.25 s)**	**Time (1.25 s)**
WO_3	17	40	71	34	81	21
WO_3/PTh	10	2	44	19	55	23
WO_3/PFu	21	28	55	12	69	24

To analyze the entire performance of the ECDs, a quality factor ($\Gamma_{(\lambda)}$) was calculated using the following equations [43]

$$\Gamma_{(\lambda)} = \frac{CE_{(\lambda)}}{\tau}, \tau = \frac{\tau_c + \tau_b}{2} \quad (3)$$

where $CE_{(\lambda)}$ is the coloration efficiency and τ_c, τ_b are the coloration and bleaching time, respectively. It stands to reason that a higher $\Gamma_{(\lambda)}$ leads to a better EC performance [43, 44]. The value of $\Gamma_{(\lambda)}$ was calculated as 43, 492, 226 $cm^2C^{-1}s^{-1}$ for ECDs based on WO_3, WO_3/PTh, and WO_3/PFu films, respectively, indicating that the electrochromic performance of the hybrid electrochromic devices is better than that of WO_3-based ECD. On the other hand, the synergic interaction between the conducting polymer (PTh or PFu) and WO_3 could lead to the formation of a p-n junction [18, 45]. In a hybrid system, the conducting polymer acts as p-type, and WO_3 acts as a n-type [18, 20]. Among hybrid ECDs, WO_3/PTh-based ECDs had the best electrochromic performance. Different electrochromic performances of hybrid ECDs can be attributed to the electron-withdrawing properties of polymers (PTh or PFu) and the aromaticity behavior of the donor types. It is well-known that furan has a higher electron withdrawing property than thiophene, and the aromaticity declines in this order, thiophene>furan, as known from previous studies [46-48].

4. CONCLUSIONS

In this study, a one-step facile preparation of plasma polymerized PTh and PFu on WO_3 powders was designed to improve electrochromic performance. The influence of chalcogen atoms (O and S) in furan and thiophene was systematically and comprehensively investigated on the electrochromic behavior of flexible film. Among flexible ECDs, a WO_3/PTh-based ECD exhibited the fastest switching speeds (τ_b: 1.63 s, τ_c: 0.41 s), the highest optical contrast (33%), the greatest coloration efficiency (502 cm^2/C), and the highest quality factor ($\Gamma_{(\lambda)}$) (492 $cm^2C^{-1}s^{-1}$), all of which can be caused by the strong synergetic effect of WO_3 and PTh. The results contribute to the demonstration that applying both RF plasma hybridization and electron beam evaporation methods produce solid-state devices for flexible EC applications that have the potential to advance flexible ECDs.

ACKNOWLEDGEMENTS

The authors gratefully acknowledge the TÜBİTAK/COST (Project No: 114M877) and Süleyman Demirel University (Project No: 4764-YL2-16) for their financial support of this study.

REFERENCES

[1] Sun S, Lu T, Chang X, Hu X, Dong L, Yin Y. Flexible electrochromic device based on $WO_3 \cdot H_2O$ nanoflakes synthesized by a facile sonochemical method. Mater Lett 2016; 185: 319–322.

[2] Lee H, Kim M, Kim I, Lee H. Flexible and stretchable optoelectronic devices using silver nanowires and graphene. Adv. Mater. 2016; 28: 4541–4548.

[3] Kim T-H, Park S-H, Kim D-H, Nah Y-C, Kim H-K. Roll-to-roll sputtered ITO/Ag/ITO multilayers for highly transparent and flexible electrochromic applications. Sol Energy Mater Sol Cells 2017; 160: 203-210.

[4] Kiristi M, Bozduman F, Oksuz A U, Oksuz L, Hala A. Solid state electrochromic devices of plasma modified WO_3 hybrids. Ind. Eng. Chem. Res. 2014; 53: 15917−15922.

[5] Xiao L, Lv Y, Dong W, Zhang N, Liu X. Dual-Functional WO_3 nanocolumns with broad band antireflective and high-performance flexible electrochromic properties. ACS Appl Mater Interfaces 2016; 8: 27107−27114.

[6] Wang S, Dou K, Zou Y, Dong Y, Li J, Ju D, Zeng H. Assembling tungsten oxide hydrate nanocrystal colloids formed by laser ablation in liquid into fast-response electrochromic films. J Colloid Interface Sci 2017; 489: 85–91.

[7] Ling H, Ding G, Mandler D, Lee PS, Xu J, Lu X. Facile preparation of aqueous suspensions of WO_3/Sulfonated PEDOT hybrid nanoparticles for electrochromic applications. Chem Commun 2016; 52: 9379-9382.

[8] Dulgerbaki C, Oksuz AU. Efficient electrochromic materials based on PEDOT/WO_3 composites synthesized in ionic liquid media. Electroanalysis 2014; 26: 2501–2512.

[9] Shirakawa H, Louis EJ, MacDiarmid AG, Chiang CK, Heeger AJ. Synthesis of electrically conducting organic polymers: halogen derivatives of Polyacetylene, (CH)x. J Chem Soc Chem Commun 1977; 0: 578-580.

[10] Chiang CK, Fincher CR, Park YW, Heeger AJ, Shirakawa H, Louis EJ, Gau SC, MacDiarmid AG. Electrical conductivity in doped Polyacetylene. Phys Rev Lett 1977; 39: 1098-1101.

[11] Chiang CK, Druy MA, Gau SC, Heeger AJ, Park YW, Shirakawa H. Synthesis of highly conducting films of derivatives of Polyacetylene, (CH)x. J Am Chem Soc 1978; 100: 1013-1015.

[12] Chiang CK, Park YW, Heeger AJ, Shirakawa H, Louis EJ, MacDiarmid AG. Conducting polymers: Halogen doped polyacetylene. Phys Rev Lett 1977; 39: 1098-1101.

[13] Hu Y, Jiang F, Lu B, Liu C, Hou J, Xu J. Free-standing oligo(oxyethylene)-functionalized polythiophene with the 3,4-ethylenedioxythiophene building block: electrosynthesis, electrochromic and thermoelectric properties. Electrochimica Acta 2017; 228: 361–370.

[14] Najafi-Ashtiani H, Bahari A, Ghasemi S. A dual electrochromic film based on nanocomposite of copolymer and WO_3 nanoparticles: Enhanced electrochromic coloration efficiency and switching response. J Electroanal Chem 2016; 774: 14–21.

[15] Kim T-H, Jeon H J, Lee J-W, Nah Y-C. Enhanced electrochromic properties of hybrid P3HT/WO_3 composites with multiple colorations. Electrochem Commun 2015; 57: 65–69.

[16] Nguyen T-T N, Chan C-Y, He J-L. One-step inkjet printing of tungsten oxide-poly(3,4-ethylenedioxythiophene): polystyrene sulphonate hybrid film and its applications in electrochromic devices. Thin Solid Films 2016; 603: 276-282.

[17] Gaikwad DK, Mali SS, Hong CK, Kadam AV. Influence of disordered morphology on electrochromic stability of WO_3/PPy. J Alloys Compd 2016; 669: 240-245.

[18] Karaca GY, Eren E, Alver C, Koc U, Uygun E, Oksuz L, Oksuz A U. Plasma modified V_2O_5/PEDOT hybrid based flexible electrochromic devices. Electroanalysis 2017; 29: 1324-1331.

[19] Oksuz A U, Manolache S, Oksuz L, Hershkowitz N. Plasma nanocoating of thiophene onto TiO_2 nanoparticles. Ind Eng Chem Res 2013; 52: 6610−6616.

[20] Dulgerbaki C, Oksuz AU. Fabricating polypyrrole/tungsten oxide hybrid based electrochromic devices using different ionic liquids. Polym Adv Technol 2016; 27: 73–81.

[21] Vos C D, Vandencasteele N, Kakaroglou A, Nisol B, Graeve I, Assche G V, Mele B V, Terryn H, Reniers F. Plasma polymerization of a saturated branched hydrocarbon. The case of heptamethylnonane. Plasma Process Polym 2013; 10: 51-59.

[22] Cools P, Geyter ND, Vanderleyden E, Barberis F, Dubruel P, Morent R. Adhesion improvement at the PMMA bone cement-titanium implant interface using methyl methacrylate atmospheric pressure plasma polymerization. Surf Coat Tech 2016; 294: 201–209.

[23] Mukherjee B, Rahman AOS, Islam A, Sribalaji M, Keshri AK. Plasma sprayed carbon nanotube and graphene nanoplatelets reinforced alumina hybrid composite coating with outstanding toughness, J Alloys Compd 2017; 727: 658-670.

[24] Zhao X-Y, Wang M-Z, Wang Z, Zhang B-Z. Structural and dielectric properties of conjugated polynitrile thin films deposited by plasma polymerization. Thin Solid Films 2008; 516:8272–8277.

[25] Shanmugapriya C, Velraj G. Investigation on structural and electrical properties of $FeCl_3$ doped polythiophene (PT) blended with micro and nano copper particles by mechanical mixing. Optik 2016; 127: 8940–8950.

[26] Gok A, Can H K, Sari B, Talu M. X-ray diffraction studies and DC electrical conductivity of poly(2-halogenanilines) and their composites with polyfuran. Mater Lett 2005; 59: 80– 84.

[27] Sen S, Bardakci B, Yavuz A G, Uygun A G. Polyfuran/zeolite LTA composites and adsorption properties. Eur Polym J 2008; 44: 2708–2717.

[28] Jiang F, Li W, Zou R, Liu Q, Xu K, An L, Hu J. MoO_3/PANI coaxial heterostructure nanobelts by in situ polymerization for high performance supercapacitors. Nano Energy 2014; 7: 72–79.

[29] Turkaslan B E, Dikmen S, Oksuz L, Oksuz A U. Plasma nanocoating of thiophene onto MoS_2 nanotubes. Appl Surf Sci 2015; 357: 1558–1564.

[30] Akpinar H Z, Udum YA, Toppare L. Spray-processable thiazolothiazole-based copolymers with altered donor groups and their electrochromic properties. J Polym Sci A Polym Chem 2013; 51: 3901–3906.

[31] Wei H, Yan X, Wu S, Luo Z, Wei S, Guo Z. Electropolymerized polyaniline stabilized tungsten oxide nanocomposite films: electrochromic behavior and electrochemical energy storage. J Phys Chem C 2012; 166: 25052−25064.

[32] Fernandes M, Leones R, Pereira S, Costa A M S, Mano J F, Silva M M, Fortunato E, Bermude V d Z. Eco-friendly sol-gel derived sodium-based ormolytes for electrochromic devices. Electrochimica Acta. 2017; 232: 484-494.

[33] Fu X, Jia C, Wan Z, Weng X, Xie J, Deng L. Hybrid electrochromic film based on polyaniline and TiO_2 nanorods array. Org Electron 2014; 15: 2702–2709.

[34] Adhikari S, Sarkar D. Synthesis and electrochemical properties of nanocuboid and nanofiber WO_3. J Electrochem Soc 2015; 162: H1-H7.

[35] Kondalkar VV, Kharade RR, Mali SS, Mane R M, Patil PB, Patil PS, Choudhury S, Bhosale PN. Nanobrick-like WO_3 thin films: Hydrothermal synthesis and electrochromic application. Superlattices Microstruct. 2014; 73: 290–295.

[36] Huang H, Tian J, Zhang W K, Gan Y P, Tao X Y, Xia X H, Tu J P. Electrochromic properties of porous NiO thin film as a counter electrode for NiO/WO_3 complementary electrochromic window. Electrochimica Acta 2011; 56: 4281–4286.

[37] Kondalkar VV, Mali SS, Kharade R R, Khot K V, Patil P B, Mane RM, Choudhury S, Patil P S, Hong CK, Kim JH, Bhosale PN. High performing smart electrochromic device based on honeycomb nanostructured h-WO_3 thin films: hydrothermal assisted synthesis. Dalton Trans 2015; 44: 2788-2800.

[38] Dulgerbaki C, Maslakci NN, Komur AI, Oksuz AU. PEDOT/WO_3 hybrid nanofiber architectures for high performance electrochromic devices. Electroanalysis 2016; 28: 1873 – 1879.

[39] Najafi-Ashtiani H, Bahari A, Ghasemi S. A dual electrochromic film based on nanocomposite of aniline and o-toluidine copolymer with tungsten oxide nanoparticles. Org Electron 2016; 37: 213-221.

[40] Kim D-M, Yoon J-H, Won M-S, Shim Y-B. Electrochemical characterization of newly synthesized polyterthiophene benzoate and its applications to an electrochromic device and a photovoltaic cell. Electrochimica Acta 2012; 67: 201– 207.

[41] Cai GF, Tu J P, Zhou D, Zhang JH, Wang XL, Gu CD. Dual electrochromic film based on WO_3/polyaniline core/shell nanowire array. Sol Energy Mater Sol Cells 2012; 122: 51–58.

[42] Zhang J, Tu J-P, Zhang D, Qiao Y Q, Xia X-H., Wang X.-L, Gu C-D. Multicolor electrochromic polyaniline–WO_3 hybrid thin films: One-pot molecular assembling synthesis. J Mater Chem 2011, 21, 17316-17324.

[43] Xiao L, Lv Y, Dong W, Zhang D, Liu X. Dual-Functional WO_3 nanocolumns with broadband antireflective and high-performance flexible electrochromic properties. ACS Appl Mater Interfaces 2016; 8: 27107−27114.

[44] Li H, Lv Y, Zhang X, Wang X, Liu X. High-performance ITO-free electrochromic films based on bi-functional stacked WO_3/Ag/WO_3 structures. Sol Energy Mater Sol Cells 2015; 136: 86–91.

[45] Zhang J, Wang S, Xu M, Wang Y, Xia H, Zhang S, Guo X, Wu S. Polypyrrole-coated SnO_2 hollow spheres and their application for ammonia sensor. J Phys Chem C 2009; 113: 1662–1665.

[46] Kavak E, Us CN, Yavuz E, Kivrak A, Özkut MI. A camouflage material: p- and n-type Dopable furan based low band gap electrochromic polymer and its EDOT based copolymer. Electrochimica Acta 2015; 182: 537–543.

[47] Karabay LC, Karabay B, Karakoy MS, Cihaner A. Effect of furan, thiophene and selenophene donor groups on benzoselenadiazole based donor-acceptor-donor systems. J electroanal chem 2016; 780: 84–89.

[48] Fringuelli F, Marino G, Taticchi A, Grandolini G. A comparative study of the aromatic character of furan, thiophen, selenophen, and tellurophen. J Chem Soc Perkin Trans 1974; 2: 332-337.